Advances in Materials Research, *Vol. 11, No. 1 (2022) 59-73*
https://doi.org/10.12989/amr.2022.11.1.059

Comparative study of finite element analysis and generalized beam theory in prediction of lateral torsional buckling

Shashi Kant Sharma*, K.V. Praveen Kumar, M. Abdul Akbar [a] and Dadi Rambabu

Department of Civil Engineering, Dr. B R Ambedkar National Institute of Technology, Jalandhar, Punjab-144011, India

(*Received May 19, 2021, Revised November 19, 2021, Accepted November 25, 2021*)

Abstract. In the construction industry, thin-walled frame elements with very slender open cross-sections and low torsional stiffness are often subjected to a complex loading condition where axial, bending, shear and torsional stresses are present simultaneously. Hence, these often fail in instability even before the yield capacity is reached. One of the most common instability conditions associated with thin-walled structures is Lateral Torsional Buckling (LTB). In this study, a first order Generalized Beam Theory (GBT) formulation and numerical analysis of cold-formed steel lipped channel beams (C80×40×10×1, C90×40×10×1, C100×40×10×1, C80×40×10×1.6, C90×40×10×1.6 and C100×40×10×1.6) subjected to uniform moment is carried out to predict pure Lateral Torsional Buckling (LTB). These results are compared with the Finite Element Analysis of the beams modelled with shell elements using ABAQUS and analytical results based on Euler's buckling formula. The mode wise deformed shape and modal participation factors are obtained for comparison of the responses along with the effect of varying the length of the beam from 2.5 m to 10 m. The deformed shapes of the beam for different modes and GBTUL plots are analyzed for comparative conclusions.

Keywords: finite element analysis; generalized beam theory; instability failure; lateral torsional buckling; light gauge steel; lipped channel beams

1. Introduction

Thin-walled structural elements, such as cold-formed steel columns or beams have many advantages and have gained popularity during the recent decades (Ádány 2019). However, these thin-walled open structures frequently fail due to instability even before reaching the yield stress and the modes of deformation associated with it are influenced by the length of the structural member and stress distribution across the cross- section (Schardt 1994). Instability condition arises when a structure starts to lose its stiffness. This can be characterized as the condition where the structural deformation corresponding to any load tends to infinite values for even the slightest increase.

Lateral Torsional Buckling (LTB) is the one of the possible modes of instability failure in laterally unsupported beams (Rossi *et al*. 2020a). It is a phenomenon in which the beam loses

*Corresponding author, Assistant Professor, E-mail: shashi.pec@gmail.com; sharmask@nitj.ac.in
[a] Assistant Professor, E-mail: akbarma@nitj.ac.in; maakbar83@yahoo.co.in

Copyright © 2022 Techno-Press, Ltd.
http://www.techno-press.org/?journal=amr&subpage=5 ISSN: 2234-0912 (Print), 2234-179X (Online)

equilibrium in the main bending plane due to lateral displacements with the addition of twist (Rossi *et al*. 2020b). Lateral Torsional Buckling comes under the category of global buckling whereas the other two buckling modes namely, local buckling and distortional buckling are known as cross-sectional buckling. In general, the deformed shape of any structural section is typically a result of cross-sectional buckling (local and distortional buckling) and rigid body displacements, which leads to a lower critical stress than the values taken individually. Incorporating the local-global interaction in the analysis is still a challenging task, mainly because of the difficulties in modeling the simultaneous short and long wave structural response. Additionally, the results obtained from numerical analyses are often difficult to process and interpret (Gonçalves *et al*. 2009). Some methods which have been adopted by the researchers are Finite Element Method, Finite Strip Method, Direct Strength Method, Codal Methods (AS/NZS4600, BS5950 PART-5, EUROCODE3-1.3, AISI method etc.), Generalized Beam Theory etc.

Generalized Beam Theory was found to be more versatile and computationally efficient method than Finite Strip Method or Finite Element Method. Nowadays, GBT is used as an efficient tool to analyze thin-walled bars undergoing combinations of global, distortional and/or local deformations. This efficiency stems from the fact that the kinematic description of the beam is based on structurally meaningful "cross-section deformation modes", which generally lead to accurate solutions when only a small number of them is included in the analysis (Manta *et al*. 2020). GBT follows a hierarchical procedure in which the solutions arise as a series of buckling modes starting from the one-dimensional beam behavior and gradually expanding to complex shell behavior. Hence, the designer gets the freedom to select the mode/modes depending on the situation under consideration. GBT describes the deformed configuration of a member as a linear combination of a set of assumed deformation modes, i.e., the degrees of freedom in GBT are modal displacements. As per conventional beam theory, there are four fundamental modes of deformation, namely extension, bending about two principal axes and torsion. These are called rigid body modes since distortions of cross-section are not involved. GBT unifies the analytical treatment of these rigid body modes and further extends it to include higher order deformation modes that involve cross-sectional distortion.

In the first order GBT, all these modes are orthogonal which implies that they are uncoupled, and their effects can be combined by simple superposition. A unifying feature of GBT is the introduction of 'warping functions' whereby each mode (k) of deformation is related with a distribution of axial strain (${}^{k}\tilde{u}$). Accordingly, for the four rigid body modes, the first mode of deformation is the axial extension, and which has a constant axial strain distribution throughout the cross-section. Hence at any point, the warping function, (${}^{k}\tilde{u} = -1$) for this mode. The second and third modes are bending about major and minor axis respectively and the warping functions linked to these modes are linear distribution of strain about the two principal axes. The final rigid body mode is torsion, and here warping function is the sectorial coordinates, which reflects the distribution of axial strain due to a moment. For a lipped Channel section, there are 6 orthogonal modes. As seen from Fig. 1, the four initial modes are rigid body modes and the higher modes (k>4) are distortional modes. For the sake of considering the effect of local buckling of flat elements between the fold lines or to increase the distortional modes, intermediate nodal points are to be added in-between the fold lines. The basic equation of GBT is Eq. (1)

$$E^k C^k V''' - G^k D^k V'' + B^k V^k = q^k \tag{1}$$

Where the forward superscript is used to represent the mode number.

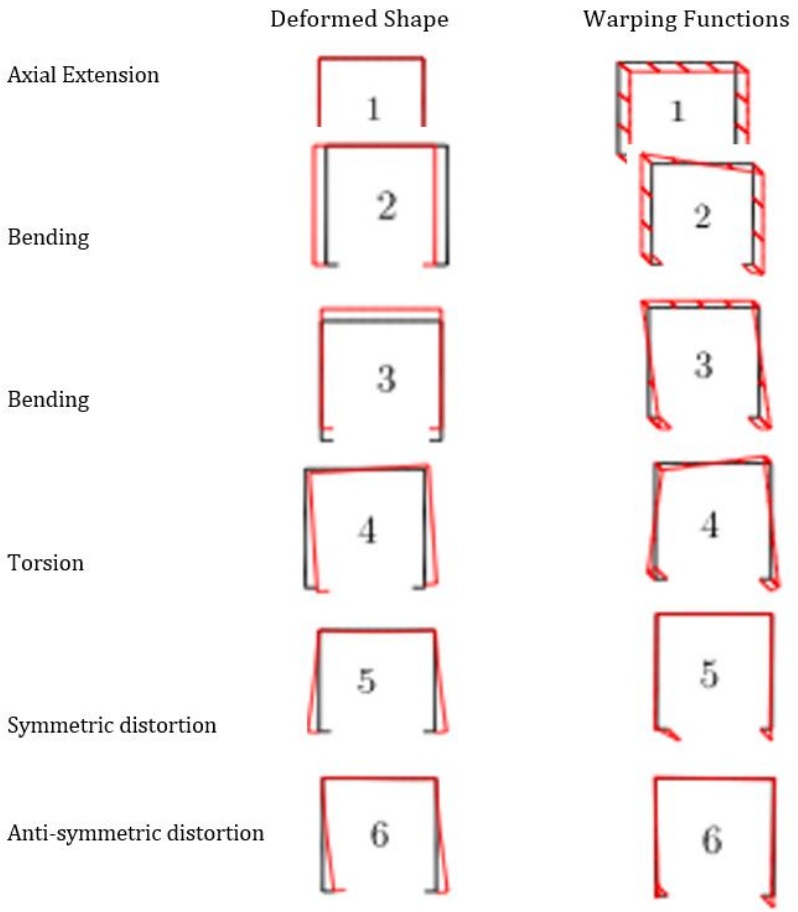

Fig. 1 Deformed shapes and warping functions for channel sections (David *et al*. 2020)

E = Modulus of elasticity
G = Shear modulus
C^k = Direct stress stiffness
D^k = Shear stress stiffness
B^k = Transverse bending stress stiffness
V^k = Generalized deformation in mode k
q^k = Distributed load corresponding to mode k

The solution of the Eq. (1) gives the stresses and deformations of the member for a specified loading and support condition. The equation can be solved in three different steps. The first step comprises of determining the warping function ($^k\tilde{ir}$) and section properties (^kC, ^kD and ^kB) corresponding to every mode (k) by considering only the cross-section. These basic section properties are further used in the solutions of fundamental GBT equation for each mode taking into account the relevant loading and boundary conditions. Once the cross-sectional properties are determined, material properties such as Modulus of elasticity (E) and Shear modulus (G) along with the support conditions, loads and length of the member are inputted into the basic equation of

Table 1 Details of channel sections

Model no.	Designation of channel section (hXbXaXt)	h (mm)	b (mm)	A (mm)	t (mm)	X_c (mm)	X_s (mm)	Area of section (mm^2)
1	C80×40×10×1	80	40	10	1	12.852	35.300	176
2	C90×40×10×1	90	40	10	1	12.63	33.824	186
3	C100×40×10×1	100	40	10	1	11.541	32.481	196
4	C80×40×10×1.6	80	40	10	1.6	11.797	32.285	267.52
5	C90×40×10×1.6	90	40	10	1.6	11.131	30.879	283.52
6	C100×40×10×1.6	100	40	10	1.6	10.537	29.605	299.52

GBT. Hence, an Eigen value problem is formed by a system of ordinary differential equations (ODEs) corresponding to each mode of deflection. The solution of this problem yields the member bifurcation stress resultants (Eigen values) and corresponding buckling mode shapes (Eigen functions). The third step involves combining the results of earlier step to calculate the required stresses and deflections. Using GBT, the stress resultant is determined as Eq. (2),

$$W^k = -E^k C^k V''' = \int \sigma^k u dA \tag{2}$$

Where, W^k is the stress resultant for mode k (e.g., bending moment for modes 2 and 3, bi moment for mode 4, etc.).

Cold-formed channels are one of the most widely used sections in construction industry lately. The channel sections can be either square or rectangular. Out of these channel sections, the most used section is the lipped rectangular channel as the lip offers sufficient flexural rigidity to maintain straightness of the edge when the element buckles on loading along with the post-buckling strength. The objective of this study is to use Generalized Beam Theory to predict the Lateral Torsional Buckling load of thin-walled (cold-formed) channel sections and to validate the results with Finite Element Analysis. Six different rectangular lipped channel sections are used for this study and the results reported is the extension of work carried out by Sharma *et al*. (2022). All the six beams are initially considered to be 2.5 m long with simply supported ends. All the models are modelled with shell elements with both of their ends torsionally restraint. Torsional restraints are provided at both ends to avoid the beams from undergoing a pure torsion under loading and in most practical applications, the ends are restrained from rotation about its own axis. All the models are laterally unsupported between the ends. The details of the cross-sections used are given in Table 1.

2. GBTUL modelling and analysis

GBTUL is a code developed by Bebiano *et al*. (2008) to solve the buckling and vibration problems of thin-walled open cross-sections. It is based on the implementation of GBT formulation so as to avoid the complex procedure of manually solving higher order differential equations involving several combinations of deformation modes. As already discussed, GBT can be considered as an elegant approach to solve several structural problems involving thin-walled

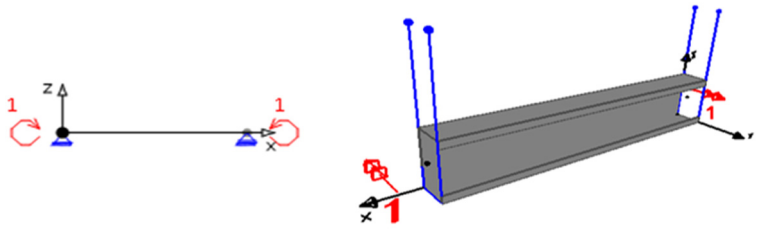

Fig. 2 Loading and support condition for buckling analysis (2D & 3D diagrams)

sections and can also be used to obtain the contributions of each deformation mode (modal participation) in the final failure mode. GBTUL 2.0 as a code (Bebiano *et al*. 2018) can only handle elastic buckling and vibration analyses of different cross-sections made of isotropic/special orthotropic materials. The GBTUL model for analysis is shown in Fig. 2.

3. Finite element analysis

The geometry of the beams was modelled in ABAQUS CAE for the Finite Element Analysis along with assignment of material properties, constraints & boundary conditions and meshing. The element used for modelling is SR4 conventional shell elements. Shell extrusion technique is used to create the geometry. Initially the cross-section profile/geometry of the beam is defined by sketching the centre line of the channel cross-section in the x-y plane and the cross-section is extruded along the z-direction to generate the complete model of the channel beam section. The beam is simply supported at the ends and the supports have to be provided at the centroid. As the centroid of a channel section lies outside the cross section, a datum point/reference node is created at the centroid on both ends and it is connected to the centre of the web using a one-dimensional beam element (B31).

The material of channel section (steel) is defined as a linear elastic with modulus of elasticity of 200000 N/mm^2 and Poisson's ratio of 0.3. The purpose of the B31 beam element is to act as a rigid connection between the centroid and beam so that there is force flow between the support and the shell elements by restricting the deflection in beam making it infinitely stiff. Hence, the material for B31 beam element is modelled with very high flexural and torsional stiffness (the moment of inertia is in the range of 10^{10} mm^4).

As the boundary condition is simply supported and the pin-roller support need to be assigned at the centroid of the cross-section, the reference point which has already been created is used. In order to ensure a uniform force flow from the cross-section to the supports, the centroid should be rigidly connected/constrained to the cross-section boundary (web, flanges and lip). This is done by using multi-point constraints (MPC). In MPC, the slave nodes (or edges) are constrained against the master node through various links. In this model, the master node is the centroid and the cross-section edges are selected as the slaves. The cross-section edges are constrained against the centroid with rigid beam links so that all the forces or displacements applied at the centroid will be transferred uniformly to the channel cross-section.

After defining the multi-point constraints, support conditions are defined at both ends of the beam. On one end, at the centroid, all the translations are arrested while at the other end, translation along the longitudinal axis (z-axis) is released and translation along the other two

directions is arrested. Since the beam is restrained against rotation, the rotational degree of freedom (DOF) about the longitudinal axis (z-axis) is arrested, while the other two rotational DOFs are released at both ends thereby stimulating a simply supported boundary condition. The loading on the beam is a constant moment applied throughout the beam about its major axis. This is simulated by applying equal and opposite moments at both ends. In order to avoid any eccentricities, the moments are applied at the centroid of the cross-section.

LTB is an instability failure and therefore in order to analyse for LTB, Eigen value analysis needs to be performed. The basic principle in Eigen value analysis is to determine the load at which the model stiffness matrix becomes singular. For this study, the analysis is carried out as linear perturbation buckling analysis using ABAQUS. Subspace iteration method is being used for extracting Eigen values. After buckling analysis, the Eigen values associated with each buckling mode starting with the first mode is obtained. These Eigen values represent the buckling load. To arrive at the actual buckling load, the Eigen values are multiplied with the applied moment. The analysis also provides the buckling mode shapes and deformed configurations. Some of the observations after analysis are as follows:

- For all the six models used in the study, the first buckling mode was Lateral Torsional Buckling as observed from the deflection diagram.
- The analysis also gave higher buckling modes. Majority of the higher buckling modes involved local buckling and distortional buckling (Fig. 3).
- The analysis also provided negative Eigen values. These are also mathematical solutions to the problem without any physical meaning. However, in this particular study, negative Eigen values and associated mode shape means that the load to cause buckling is of the opposite sign as compared to the applied load i.e., if the load was applied in the opposite direction to the actual case, the beam would have buckled in the respective mode shape.

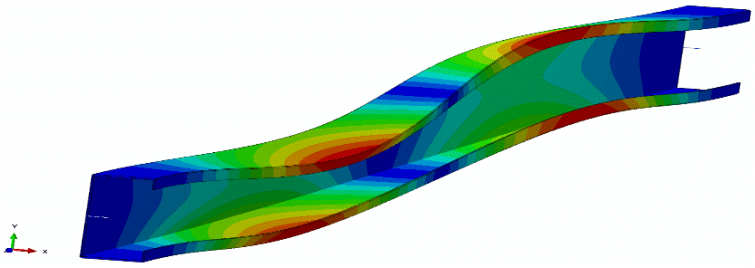

Fig. 3 Analysed model in ABAQUS (C80×40×10×1.6)

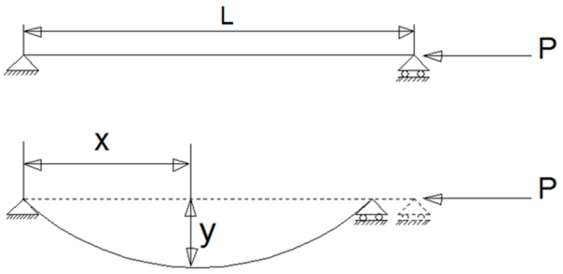

Fig. 4 Pure buckling of beam under compression

Table 2 Comparison of GBTUL critical buckling loads with theoretical buckling values

Model no.	Designation of channel section (*h*X*b*X*a*X*t*)	GBTUL (kN)	ABAQUS (kN)	Theoretical buckling value (kN)
1	C80×40×10×1	13.457	13.415	13.5
2	C90×40×10×1	13.979	13.943	14.001
3	C100×40×10×1	14.443	14.365	14.486
4	C80×40×10×1.6	21.562	21.498	21.561
5	C90×40×10×1.6	22.409	22.376	22.412
6	C100×40×10×1.6	23.168	23.064	23.178

- Buckling modes involving interactions between global and local buckling effects were also obtained at higher modes.

Theoretical buckling load for a beam (Fig. 4) under compression is calculated using Euler's buckling load formula.

Euler's Critical buckling load for the section C80×40×10×1.6 of modulus of elasticity (E = 200000 N/mm^2), moment of inertia about minor axis (I = 68337.58 mm^4), Effective length (L = 2500 mm) is calculated as follows

$$P_{cr(theoretical)} = \frac{\pi^2 EI}{L^2} = \frac{\pi^2 * 200000 * 68337.58}{2500^2} \tag{3}$$

The comparison of buckling loads calculated from the GBTUL model, ABAQUS model and theoretical approach is shown in Table 2. As seen, the difference between modelling and theoretical values is less than 0.85% for all cases. Thus, the buckling loads obtained from GBTUL models and theoretical buckling loads are comparable. This is an indication that the geometry, material property and boundary conditions have been modelled properly in GBTUL and hence the results obtained can be used for the comparative study. Earlier researchers have also obtained validation of GBT results by comparison with values obtained with Finite Element Analysis modelled using shell elements (Nedelcu and Mureşan 2017).

4. Results and discussion

In this study, six cold-formed steel channel sections were analyzed to determine the critical buckling load. Based on the results, a comparison is carried out between the buckling analysis results obtained from two different numerical analysis techniques (FEM and GBT). Since the study deals with an instability failure problem and follows Eigen value analysis, the comparison of first three Eigen modes is given here. The participation of each individual mode contributing to the failure corresponding to each Eigen mode is also obtained from GBTUL analysis. By checking the modal participation and deflected shape of the beam, the type of failure can be understood, whether it is Lateral Torsional Buckling or distortional. All the sections are of 2.5 m length and analysed under a uniform/constant moment load. Table 3 gives the comparison of critical buckling loads obtained from ABAQUS and GBTUL for channels C80×40×10×1, C90×40×10×1 and C100×40×10×1. Table 4 gives the modal participation (in percentage) for those sections.

Table 3 Comparison of critical buckling loads from ABAQUS and GBTUL analysis (1 mm thick sections)

Sl. No.	Channel section	Critical buckling moment (kNm)					
		Eigen value 1		Eigen value 2		Eigen value 3	
		ABAQUS	GBTUL	ABAQUS	GBTUL	ABAQUS	GBTUL
1	C80×40×10×1	1.136	0.556	1.97	1.91	1.98	1.99
2	C90×40×10×1	1.312	0.63	2.17	2.18	2.18	2.23
3	C100×40×10×1	1.488	0.706	2.37	2.37	2.38	2.43

Table 4 Modal participation for corresponding Eigen modes (1 mm thick sections)

Sl. no.	Channel section	Eigen mode no.	Modal participation (%)					
			Axial	Bending (major)	Bending (minor)	Torsion	Symmetric distortion	Anti-symmetric distortion
1	C80×40×10×1	EM 1	0	0	50	50	0	0
		EM 2	0	0	43	50	7	0
		EM 3	0	0	0	3	50	47
2	C90×40×10×1	EM 1	0	0	50	50	0	0
		EM 2	0	0	0	2	50	48
		EM 3	0	0	0	1.5	50	48.5
3	C80×40×10×1	EM 1	0	0	50	50	0	0
		EM 2	0	0	0	1	50	49
		EM 3	0	0	0	1	50	49

From Table 4, it can be observed that for all the sections, first mode of failure is contributed by 50% bending about minor axis (buckling) and 50% torsion which represents the global buckling failure mode of LTB (Lateral Torsional Buckling). In the second Eigen mode, distortion also contributes to the failure. The lowest buckling load (first Eigen value) in all the cases corresponds to LTB mode. The critical buckling load obtained for the first failure mode from FEM and GBT analyses differ greatly with each other. All the values obtained from ABAQUS are almost twice as that of GBTUL critical loads (Table 3). In the subsequent modes, critical loads obtained from both the analyses were comparable with a maximum percentage difference of 3%. Plots showing the variation of critical buckling load obtained from the two analyses are given in Fig. 5.

Deflected shapes of C80×40×10×1 channel section corresponding to first Eigen mode are compared in Figs. 6(a) and (b). From the modal participation values shown in Table 2 and the deflection diagrams obtained from ABAQUS and GBTUL, it is clear that the first mode of buckling corresponds to Lateral Torsional Buckling. Even if the critical buckling load obtained varies from each other, the deflected diagrams confirm that the first mode of buckling in thin-walled steel sections under a uniform/constant moment is LTB. It is inferred that this is likely due to pre buckling stress state not being uniform, with stress concentrations appearing near the member ends (Giovanni *et al*. 2016).

The support condition chosen for the analysis was simply supported but the options to simulate support conditions with an additional restrained/free degree of freedom are not available in

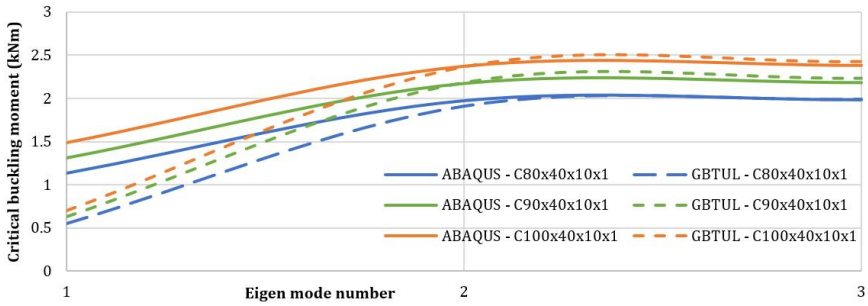

Fig. 5 Comparison of ABAQUS and GBTUL critical buckling loads (1 mm thick sections)

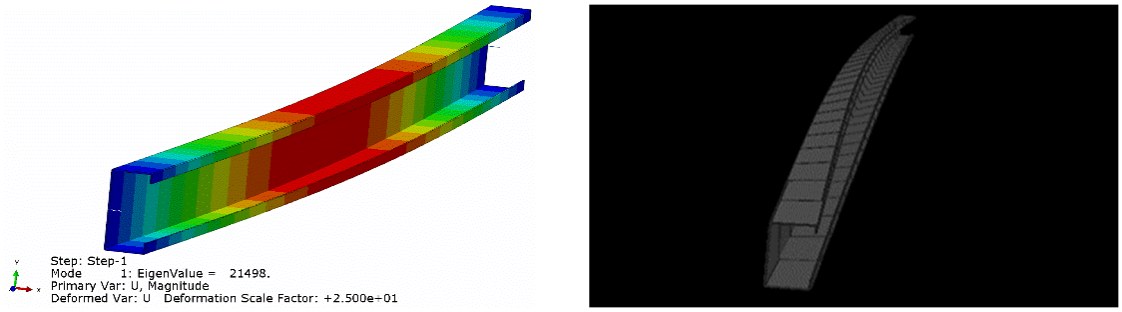

(a) ABAQUS (b) GBTUL

Fig. 6 Comparison of ABAQUS and GBTUL critical buckling loads (1 mm thick sections)

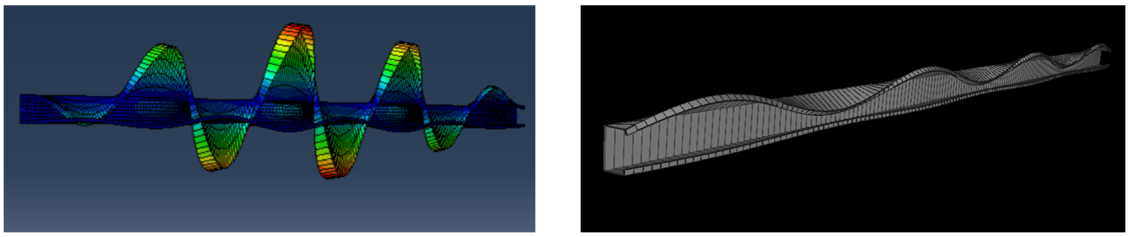

(a) ABAQUS (b) GBTUL

Fig. 7 Deflected shapes of C80×40×10×1 beam in third Eigen mode

GBTUL as of now. However, in ABAQUS the actual simulation of the support condition is done i.e., simply supported with torsional restraints and multi-point constraints to get the uniform distribution of loads. The disparity in critical buckling load in first Eigen mode which does not involve distortion (i.e., only involving rigid body deformation modes) and changes in deflected shapes can be due to this modelling difference. When the distortion comes into picture, the critical buckling loads and deflection diagrams obtained are similar. The deflection diagram for failure modes involving distortion is given in Figs. 7(a) and (b).

Upon compression of C80×40×10×1.6, C90×40×10×1.6 and C100×40×10×1.6, it is seen that unlike sections with 1 mm thickness (slenderer), the buckling loads for these sections show considerable difference up to second Eigen mode (Table 5). This can be due to the modelling

Table 5 Comparison of critical buckling load values from ABAQUS and GBTUL analysis (1.6 mm thick sections)

Sl. No.	Channel section	Critical buckling moment (kNm)					
		Eigen value 1		Eigen value 2		Eigen value 3	
		ABAQUS	GBTUL	ABAQUS	GBTUL	ABAQUS	GBTUL
1	C80×40×10×1.6	1.92	1.02	4.82	3.34	5.33	5.47
2	C90×40×10×1.6	2.19	1.14	5.6	3.82	5.9	6.01
3	C100×40×10×1.6	2.47	1.26	6.385	4.33	6.44	6.56

Table 6 Modal participation for corresponding Eigen modes (1.6 mm thick sections)

Sl. no.	Channel section	Eigen mode no.	Modal participation (%)					
			Axial	Bending (major)	Bending (minor)	Torsion	Symmetric distortion	Anti-symmetric distortion
1	C80×40×10×1.6	EM 1	0	0	50	50	0	0
		EM 2	0	0	50	47	3	0
		EM 3	0	0	0	3	50	47
2	C90×40×10×1.6	EM 1	0	0	50	50	0	0
		EM 2	0	0	48	50	2	0
		EM 3	0	0	0	2	48	50
3	C100×40×10×1.6	EM 1	0	0	50	50	0	0
		EM 2	0	0	48	50	2	0
		EM 3	0	0	0	1	50	49

difference as mentioned earlier. However, like the earlier findings, this disparity in values is present only when the failure mode is contributed solely by the rigid body deformations (Table 6). When distortions are involved, the values obtained are the same with less than 3% difference (Table 5 and Fig. 8).

Deflection diagrams for the section C80×40×10×1.6 corresponding to first Eigen mode are given in Figs. 8(a) and (b). Similar to previous sections, the first mode is LTB, which can be interpreted from the modal participation values and the deflection diagrams. In these sections, the distortion is relatively negligible in the second Eigen mode compared to the previous sections with 1 mm thickness. When the distortion mode is predominant, the critical loads and deflection diagrams obtained from ABAQUS and GBTUL are found to be comparable (Fig. 9). Hence, one of the important observations is that when the rigid body deformations are predominant in the final failure mode, the critical buckling load values obtaining from GBT are considerably lower than those obtained from FEM analysis.

One of the most important factors which can influence the critical buckling load of a beam is its slenderness ratio which is directly proportional to its length. The earlier parts of this section presented the critical buckling load corresponding to LTB for simply supported channel sections 2.5 m long. Here the variation of critical buckling load corresponding to LTB with the increase in length is presented for all cross-sections under consideration (Table 7). The plots showing the

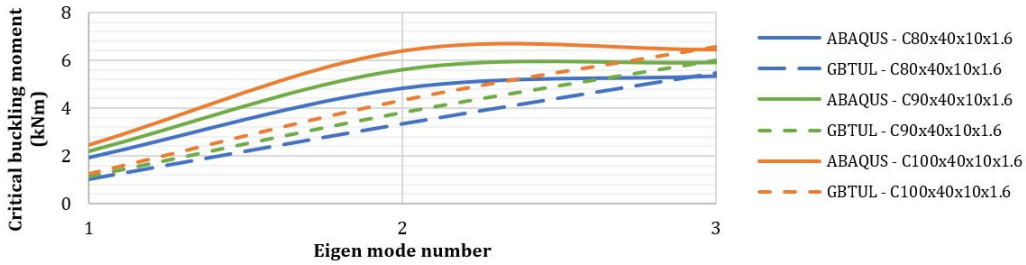

Fig. 8 Comparison of ABAQUS and GBTUL critical buckling loads (1.6 mm thick sections)

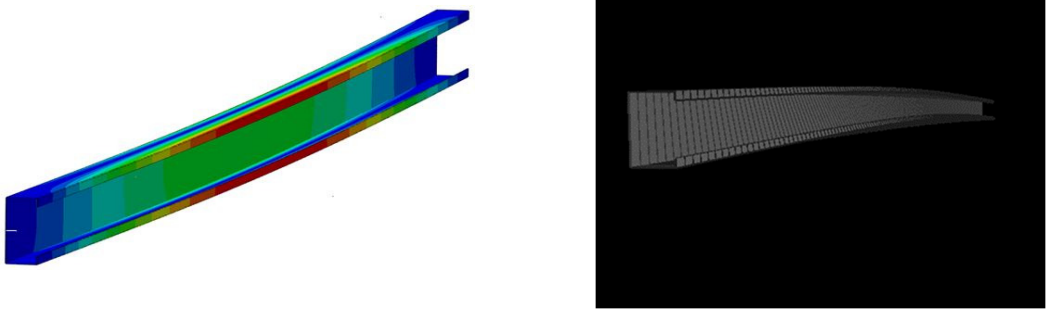

(a) ABAQUS (b) GBTUL

Fig. 9 Comparison of ABAQUS and GBTUL critical buckling loads (1.6 mm thick sections)

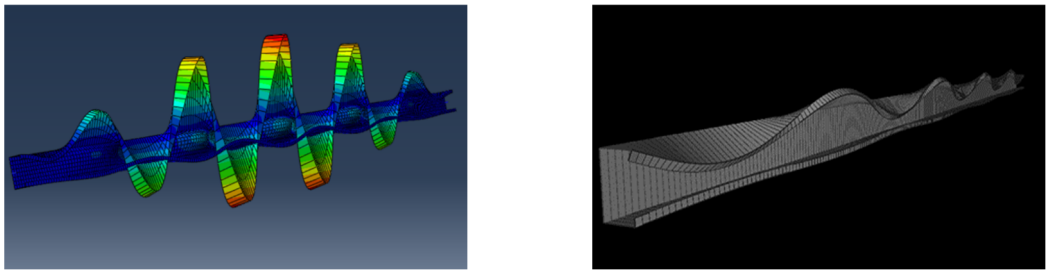

(a) ABAQUS (b) GBTUL

Fig. 10 Deflected shapes of C80×40×10×1.6 beam in third Eigen mode

variation of critical buckling loads (Fig. 10) and modal participation diagram (Fig. 11) for changing lengths are also given.

From Table 7 and Fig. 11, it is clear that the critical buckling load shows a significant decrease with increase in length in the first Eigen mode for all the sections under consideration. It can be compared to the case of column buckling under axial load since the critical buckling load shows a similar variation with increase in height of column (Euler's Buckling Theory). However, for all the channel sections under consideration, the first Eigen mode of failure is found to be Lateral Torsional Buckling (LTB) under uniform/constant moment irrespective of the length. This can be confirmed from the modal participation diagram (Fig. 12) obtained from GBTUL analysis for

Table 7 Modal participation for corresponding Eigen modes

Sl. no	Channel section	Critical buckling moment (kNm) for different length, L			
		Eigen Value 1			
		L = 2.5 m	L = 5 m	L = 7.5 m	L = 10 m
1	C80×40×10×1	0.56	0.18	0.10	0.07
2	C90×40×10×1	0.63	0.19	0.11	0.07
3	C100×40×10×1	0.71	0.21	0.12	0.08
4	C80×40×10×1.6	1.02	0.38	0.23	0.17
5	C90×40×10×1.6	1.14	0.41	0.25	0.18
6	C100×40×10×1.6	1.26	0.44	0.26	0.19

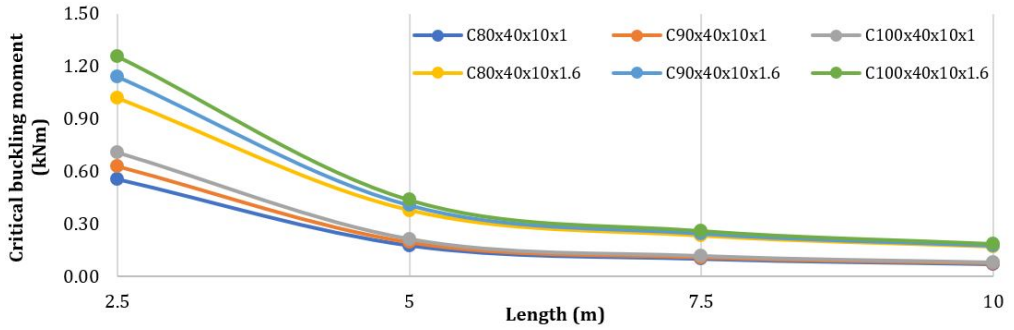

Fig. 11 Modal participation diagram for first Eigen mode

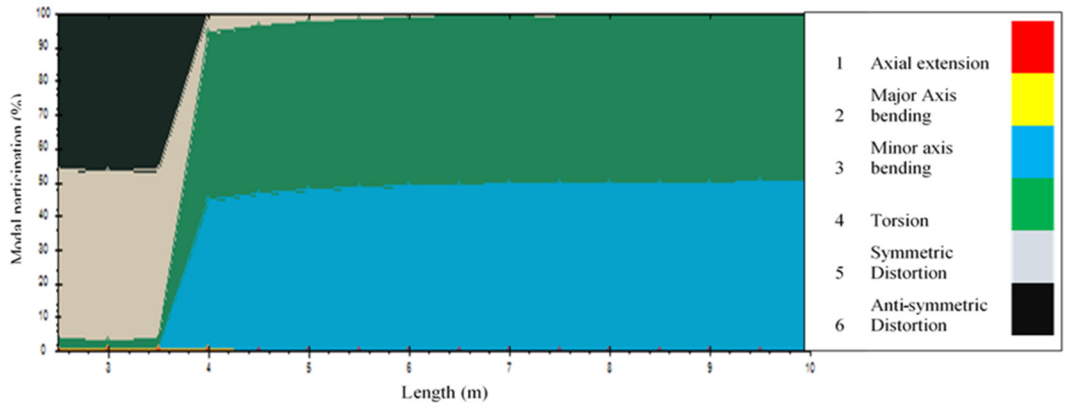

Fig. 12 Modal participation diagram (C80×40×10×1) for third Eigen mode

lengths varying from 2.5 m to 10 m. For all the lengths, it was observed that the first mode is solely contributed by minor axis bending (50%) and torsion (50%). However, the modal participation diagram for 3rd Eigen mode in general shows that for shorter lengths upto 3.5 m, the failure mode is mainly contributed by distortion modes but for beams longer than 4 m, the most critical failure mode is torsional buckling (Fig. 12).

5. Conclusions

This study reports the results of buckling analysis of thin-walled lipped channel sections using GBT and its subsequent FEM analysis using ABAQUS for a constant/uniform moment load. Based on the study, following general conclusions have been made:

- The critical buckling loads corresponding to LTB obtained from GBT analysis is almost half (46%-52% lesser) of the values that are obtained from FEM analysis. The modal participation values (from GBTUL) shows that the failure is solely contributed by torsion (50%) and buckling (50%) and the deflection diagrams obtained from both the analyses confirm the occurrence of LTB. Hence a conservative LTB prediction is done by GBT rather than FEM or in other words FEM overestimates the critical buckling value corresponding to LTB.
- When the distortions (symmetric and anti-symmetric) are majorly involved in the final failure mode, the critical buckling values are found to be comparable with less than 3% difference. The deflection diagrams are also found to be similar. Hence, both the methods are equally reliable in predicting failure modes majorly involving distortion.
- The buckling analysis of channel sections under axial load using FEM and GBT techniques give critical buckling loads marginally close to the Euler's buckling load with a maximum percentage difference of 0.3% and 0.8% respectively.
- For all the sections under consideration with 1 mm thickness, in the third mode of failure, distortion is the governing mode of deformation till 3.5 m beam length and LTB is the governing mode for lengths greater than 4 m. For sections with 1.6 mm thickness, governing mode is distortion up to 2.5 m length and for beams longer than 3 m, LTB is the governing mode.

Based on the investigation, LTB is found to be the most critical global buckling phenomena (instability failure) for all the channel sections under consideration in both the analysis methods followed i.e., GBT and FEM. The critical buckling loads obtained from GBT corresponding to LTB are considerably lower than that obtained from FEM analysis. GBT provides a better interpretation of the final failure mode with the help of modal participation values. The participation percentage of torsion, buckling and distortions obtained in each mode could explain the deflection diagram obtained from ABAQUS. Considering the significance and additional insights provided by GBT, there is a need for increased research attention and wider adoption of its results in industrial practices and design codes.

References

Adany, S. (2019), "Modal identification of thin-walled members by using the constrained finite element method", *Thin-Wall. Struct.*, **140**, 31-42. https://doi.org/10.1016/j.tws.2019.03.029

Anbarasu, M. (2016), "Local-distortional buckling interaction on cold-formed steel lipped channel beams", *Thin-Wall. Struct.*, **98**, 351-359. https://doi.org/10.1016/j.tws.2015.10.003

Basaglia, C. and Camotim, D. (2015), "Buckling analysis of thin-walled steel structural systems using generalized beam theory (GBT)", *Int. J. Struct. Stabil. Dyn.*, **15**(1), 1-28. https://doi.org/10.1142/S0219455415400040

Basaglia, C., Camotim, D. and Silvestre, N. (2009), "GBT-based local, distortional and global buckling analysis of thin-walled steel frames", *Thin-Wall. Struct.*, **47**(11), 1246-1264.

https://doi.org/10.1016/j.tws.2009.04.003
Bebiano, R., Silvestre, N. and Camotim, D. (2008), "GBTUL - A code for the buckling analysis of cold-formed steel members", *Proceedings of the 19th International Specialty Conference on Recent Research and Developments in Cold-Formed Steel Design and Construction*, St. Louis, MO, USA, October, pp. 61-79.
Bebiano, R., Camotim, D. and Gonçalves, R. (2018), "GBTUL 2. 0 − A second-generation code for the GBT-based buckling and vibration analysis of thin-walled members", *Thin-Wall. Struct.*, **124**, 235-257. https://doi.org/10.1016/j.tws.2017.12.002
Collin, P., Möller, M. and Johansson, B. (1998), "Lateral-torsional buckling of continuous bridge girders", *J. Constr. Steel Res.*, **45**(2), 217-235. https://doi.org/10.1016/S0143-974X(97)00063-1
David, M., Rodrigo, G. and Dinar, C. (2020), "Combining shell and GBT-based finite elements: Linear and bifurcation analysis", *Thin-Wall. Struct.*, **152**, 1-14. https://doi.org/10.1016/j.tws.2020.106665
Davies, J.M. and Leach, P. (1992), "Some applications of generalized beam theory", In: *Session 08*: *Special Analysis and Current Research*, pp. 479-501.
Davies, J.M. and Leach, P. (1994), "First-order generalised beam theory", *J. Constr. Steel Res.*, **31**(2-3), 187-220. https://doi.org/10.1016/0143-974X(94)90010-8
Davies, J.M., Leach, P. and Heinz, D. (1994), "Second-order generalised beam theory", *J. Constr. Steel Res.*, **31**(2-3), 221-241. https://doi.org/10.1016/0143-974X(94)90011-6
Dolamune, K.N. and Mahendran, M. (2012), "Behaviour and design of cold-formed steel beams subject to lateral–torsional buckling", *Thin-Wall. Struct.*, **51**, 25-38. https://doi.org/10.1016/j.tws.2011.10.012
Erkmen, R.E. and Attard, M.M. (2011), "Lateral-torsional buckling analysis of thin-walled beams including shear and pre-buckling deformation effects", *Int. J. Mech. Sci.*, **53**(10), 918-925. https://doi.org/10.1016/j.ijmecsci.2011.08.006
Giovanni, G., Rodrigo, G., Antonio, B., David, M., Rui, B., Leonardo, L., Domenico, M. and Dinar, C. (2016), "Deformation modes of thin-walled members: A comparison between the method of Generalized Eigenvectors and Generalized Beam Theory", *Thin-Wall. Struct.*, **100**, 192-212. http://dx.doi.org/10.1016/j.tws.2015.11.013
Gonçalves, R. and Camotim, D. (2007), "Thin-walled member plastic bifurcation analysis using generalised beam theory", *Adv. Eng. Software*, **38**(8-9), 637-646. https://doi.org/10.1016/j.advengsoft.2006.08.027
Gonçalves, R. and Camotim, D. (2012), "Geometrically non-linear Generalised Beam Theory for elastoplastic thin-walled metal members", *Thin-Wall. Struct.*, **51**, 121-129. https://doi.org/10.1016/j.tws.2011.10.006
Gonçalves, R., Dinis, P.B. and Camotim, D. (2009), "GBT formulation to analyse the first-order and buckling behaviour of thin-walled members with arbitrary cross-sections", *Thin-Wall. Struct.*, **47**(5), 583-600. https://doi.org/10.1016/j.tws.2008.09.007
Kasiviswanathan, M. and Anbarasu, M. (2021), "Simplified approach to estimate the lateral torsional buckling of GFRP channel beams", *Struct. Eng. Mech., Int. J.*, **77**(4), 523-533. http://doi.org/10.12989/sem.2021.77.4.523
Manta, D., Gonçalves, R. and Camotim, D. (2020), "Combining shell and GBT-based finite elements: Linear and bifurcation analysis", *Thin-Wall. Struct.*, **152**, 106665. https://doi.org/10.1016/j.tws.2020.106665
Mehri, H., Crocetti, R. and Gustafsson, P.J. (2015), "Unequally spaced lateral bracings on compression flanges of steel girders", *Structures*, **3**, 236-243. https://doi.org/10.1016/j.istruc.2015.05.003
Michal, J.D. (1992), "Some applications of generalized beam theory", *Proceedings of the 11th International Specialty Conference on Cold-Formed Steel Structures*, pp. 479-501.
Mohammad, R., Amir, RM. and Ali, A. (2018), "Lateral-torsional buckling of functionally graded tapered I-beams considering lateral bracing", *Steel Compos. Struct., Int. J.*, **28**(4), 403-414. http://doi.org/10.12989/scs.2018.28.4.403
Nandini, P. and Kalyanaraman, V. (2010), "Strength of cold-formed lipped channel beams under interaction of local, distortional and lateral torsional buckling", *Thin-Wall. Struct.*, **48**(10-11), 872-877. https://doi.org/10.1016/j.tws.2010.04.013
Nedelcu, M. and Mureşan, A.A. (2017), "GBT-based Finite Element formulation for elastic buckling

analysis of conical shells", *Special Issue*: *Proceedings of Eurosteel 2017*, 1(2-3), 1381-1389. https://doi.org/10.1002/cepa.180

Nguyen, C.T., Moon, J., Le, V.N. and Lee, H.E. (2010), "Lateral-torsional buckling of I-girders with discrete torsional bracings", *J. Constr. Steel Res.*, **66**(2), 170-177. https://doi.org/10.1016/j.jcsr.2009.09.011

Nguyen, C.T., Joo, H.S., Moon, J. and Lee, H.E. (2012), "Flexural-torsional buckling strength of I-girders with discrete torsional braces under various loading conditions", *Eng. Struct.*, **36**, 337-350. https://doi.org/10.1016/j.engstruct.2011.12.022

Rossi, A., Carlos, H.M., Nicoletti, R.S. and desouza, A.S.C. (2020a), "Reassesment of lateral torsional buckling in hot-holled I-beams", *Structures*, **26**, 524-536. https://doi.org/10.1016/j.istruc.2020.04.041

Rossi, A., Ferreira, F.P.V., Carlos, H.M. and Junior, E.C.M. (2020b), "Assessment of lateral distortional buckling resistance in welded I-beams", *J. Constr. Steel Res.*, **166**, 105924. https://doi.org/10.1016/j.jcsr.2019.105924

Roy, K., Ting, T.C.H., Lau, H.H. and Lim, J.B.P. (2018), "Nonlinear behavior of axially loaded back-to-back built-up cold-formed steel un-lipped channel sections", *Steel Compos. Struct.*, *Int. J.*, **28**(2), 233-250. http://doi.org/10.12989/scs.2018.28.2.233

Roy, K., Ting, T.C.H., Lau, H.H. and Lim, J.B.P. (2019), "Finite element modelling of back-to-back built-up cold-formed stainless-steel lipped channels under axial compression", *Steel Compos. Struct.*, *Int. J.*, **33**(1), 37-66. http://doi.org/10.12989/scs.2018.28.2.233

Schardt, R. (1994), "Generalized beam theory-an adequate method for coupled stability problems", *Thin-Wall. Struct.*, **19**(2-4), 161-180. https://doi.org/10.1016/0263-8231(94)90027-2

Selcuk, B. (2019), "Lateral torsional buckling of steel I-beams: Effect of initial geometric imperfection", *Steel Compos. Struct.*, *Int. J.*, **30**(5), 483-492. http://doi.org/10.12989/scs.2019.30.5.483

Sharma, S.K., Kumar, K.V.P., Akbar, M.A. and Rambabu, D. (2022), "Application of Generalised Beam Theory in Predicting Lateral Torsional Buckling of Thin-Walled Steel Sections", *Proceedings of SECON'21. Lecture Notes in Civil Engineering*, 171. https://doi.org/10.1007/978-3-030-80312-4_4

Yuan, W. and Nan, S. (2019), "An Analytical Solution of Local – Global Interaction Buckling of Cold - Formed Steel Channel - Section Columns", *Int. J. Steel Struct.*, **19**(5), 1578-1591. https://doi.org/10.1007/s13296-019-00232-4

Yura, J.A. (2001), "Fundamentals of beam bracing", *Eng. J.*, **38**(1), 11-26.

CC